Intermetallics 42 (2013) 9–13

Contents lists available at SciVerse ScienceDirect

Intermetallics

journal homepage: www.elsevier.com/locate/intermet

Corrosion behavior and mechanical properties of Mg–Zn–Ca amorphous alloys

Fengxiang Qin*, Guoqiang Xie, Zhenhua Dan, Shengli Zhu, Ichiro Seki

Institute for Materials Research, Tohoku University, 980-8577 Sendai, Japan

ARTICLE INFO

Article history:
Received 21 December 2012
Received in revised form
24 April 2013
Accepted 30 April 2013
Available online

Keywords:
B. Corrosion
B. Glasses, metallic
F. Mechanical testing
G. Biomedical applications

ABSTRACT

In this research, the corrosion behavior and mechanical properties of the Mg–Zn–Ca amorphous alloys, as well as the effects of Ag addition were investigated. The results revealed that the as-cast $Mg_{65}Zn_{30}Ca_5$ amorphous alloy exhibited the high fracture strength over 720 MPa, which was further enhanced by 1% Ag addition. The polarization resistances in Hanks' solution of high purity Mg, $Mg_{65}Zn_{30}Ca_5$, $Mg_{65}Zn_{30}Ca_4Ag_1$ and $Mg_{63}Zn_{30}Ca_4Ag_3$ amorphous alloys were 5710, 5640, 8542 and 4125 Ohms/cm^2, respectively. The minor addition of 1% Ag and homogeneous structure are responsible for improved strength and polarization resistance. With more Ag addition, both the strength and corrosion resistance were decreased due to the deceasing of the glass forming ability and galvanic corrosion.

1. Introduction

The high reactivity of Mg alloys in corrosive media can be utilized as an advantage in biomedical applications, particularly in temporary implants, although it is regarded as a major drawback when they are utilized as structural materials. Mg exists in a large amount in human body, involving in kinds of metabolic reactions and physiological mechanisms. Mg ions are essential to the basic nucleic acid chemistry of life, and thus are essential to all cells of all known living organisms. Comparing with Co, Ti or stainless steel implant materials, it has many advantages such as the low density and low Young's modulus. The density of Mg (1.74 g/cm^3) is similar to that of natural bone (1.75–2.10 g/cm^3). The elastic modulus of magnesium alloys (41–45 GPa) is much closer to that of natural bones (10–30 GPa) in comparison with that of Ti alloys (~110 GPa), stainless steels (~200 GPa), and Co–Cr alloys (~230 GPa). Therefore, Mg and Mg alloys are recently in great interest to be used as biodegradable implant materials, such as cardiovascular or orthopedic devices [1,2]. So far series of Mg–Al–Zn [3–5], Mg–Ca [6,7], Mg–Zn [8,9], Mg–Zn–Mn [10,11], Mg–Zn–Ca [12,13] alloys have been developed as biodegradable materials. Among them, one of Mg-based bulk amorphous alloys, containing the essential elements Zn and Ca for humans, has been studied with reference to biosafety and biocompatibility of released alloying elements [12–14].

Mg–Zn–Ca bulk amorphous alloys exhibited three times of the strength of pure Mg [15], noble corrosion potentials, reduced current densities and higher cell viabilities compared with as-rolled pure Mg. It was also reported that hydrogen evolution was greatly reduced by using of Mg–Zn–Ca amorphous alloys, which showed only marginal hydrogen evolution during in vitro and in vivo degradation [14]. Although some researching works have been published on Mg-based alloys [12–15], the poor mechanical properties and corrosion resistance limit the clinical application of them. The aims of this research are to improve the mechanical properties and to decrease the degradation rate of Mg–Zn–Ca amorphous alloys. The mechanical properties at room temperature and corrosion behavior in Hanks' solution at 310 K of the Mg–Zn–Ca amorphous alloy, as well as the effects of Ag addition were investigated.

2. Experimental procedures

Master alloys with nominal compositions of $Mg_{65}Zn_{30}Ca_5$, $Mg_{65}Zn_{30}Ca_4Ag_1$ or $Mg_{63}Zn_{30}Ca_4Ag_3$ (a.t.%) were prepared by melting the mixture of pure elements of Mg (99.95 wt%), Ca (99.99 wt%), Zn (99.99 wt%) and Ag (99.99 wt%) in an induction furnace under the Ar gas atmosphere. The amorphous ribbons with 3 mm in width and 35 μm in thickness were produced by melt spinning. The rod samples with a diameter of 2 mm were prepared

* Corresponding author. Tel.: +81 22 2152592; fax: +81 22 2152381.
E-mail address: fxqin@imr.tohoku.ac.jp (F. Qin).

0966-9795/$ – see front matter © 2013 Elsevier Ltd. All rights reserved.
http://dx.doi.org/10.1016/j.intermet.2013.04.021

by injection casting into a copper mold. The structure of the as-prepared ribbons and rod samples was verified by X-ray diffraction with Cu Kα radiation (Rigaku, RINT-Ultima III). Thermal stability was examined by differential scanning calorimetry (DSC, Q100) at a heating rate of 40 K/min. Uniaxial compression testing was conducted with a conventional mechanical testing machine at room temperature. The initial strain rate was 5×10^{-4} s^{-1}. The cylindrical test samples with 2 mm in diameter and 4 mm in height were used, and the ends were polished carefully to ensure parallelism. At least three specimens for each condition were tested to get a statistical result. The corrosion behavior of the samples was evaluated by electrochemical measurements. Electrolyte was simulated body fluid of Hanks' solution with pH 7.4 at 310 K open to air, which was prepared from reagent grade chemicals and deionized water. The composition of Hanks' solution (g/L) is 8.00 NaCl, 0.40 KCl, 0.35 $NaHCO_3$, 0.19 $CaCl_2 \cdot 2H_2O$, 0.09 $Na_2HPO_4 \cdot 7H_2O$, 0.2 $MgSO_4 \cdot 7H_2O$, 0.06 KH_2PO_4 and 1.00 Glucose. Electrochemical measurements were conducted in a three-electrode cell using a platinum counter electrode and an Ag/AgCl reference electrode. Potentiodynamic polarization curves were measured with a potential sweep rate of 1 mV/s. The analysis of the chemical bonding state of the samples was conducted by an X-ray photoelectron spectrometer (XPS, Shimadzu Kratos, AXIS-Ultra DLD) with monochromatized Al Kα excitation (hυ = 1486.6 eV).

3. Results and discussion

The XRD patterns of the as-spun $Mg_{65}Zn_{30}Ca_5$, $Mg_{65}Zn_{30}Ca_4Ag_1$ and $Mg_{63}Zn_{30}Ca_4Ag_3$ ribbons are shown in Fig. 1. A halo peak appears in the XRD pattern of the as-spun ribbons, demonstrating that the as-spun ribbons are mainly amorphous structure. Fig. 2 is the DSC curves of the as-spun $Mg_{65}Zn_{30}Ca_5$, $Mg_{65}Zn_{30}Ca_4Ag_1$ and $Mg_{63}Zn_{30}Ca_4Ag_3$ ribbons. The $Mg_{65}Zn_{30}Ca_5$ ribbon shows a distinct glass transition temperature (T_g) of 413 K, and an onset temperature of crystallization (T_x) of 430 K, following by a multiple crystallization process. $Mg_{65}Zn_{30}Ca_4Ag_1$ and $Mg_{63}Zn_{30}Ca_4Ag_3$ ribbons have a multiple crystallization process which is similar as that of $Mg_{65}Zn_{30}Ca_5$ alloy, while the glass transition point is unintelligible.

Fig. 3 exhibits polarization curves of as-spun $Mg_{65}Zn_{30}Ca_5$, $Mg_{65}Zn_{30}Ca_4Ag_1$ and $Mg_{63}Zn_{30}Ca_4Ag_3$ ribbons in Hanks' solution at 310 K. The data of high purity Mg is also shown for comparison. $Mg_{65}Zn_{30}Ca_5$, $Mg_{65}Zn_{30}Ca_4Ag_1$ and $Mg_{63}Zn_{30}Ca_4Ag_3$ alloys exhibit an open-circuit potential about 460–510 mV higher than that of high purity Mg, hinting the increasing of the chemical stability with addition of Zn, Ca or Ag alloying elements. $Mg_{65}Zn_{30}Ca_5$ dissolves actively with a high current density when the potential is high than open-circuit potential. The current density of $Mg_{65}Zn_{30}Ca_4Ag_1$ or $Mg_{63}Zn_{30}Ca_4Ag_3$ ribbon is lower than that of $Mg_{65}Zn_{30}Ca_5$ during the process of anodic polarization and a short passive-like region appears in the curves of $Mg_{65}Zn_{30}Ca_4Ag_1$. $Mg_{65}Zn_{30}Ca_4Ag_1$ and $Mg_{63}Zn_{30}Ca_4Ag_3$ are anodically less active and cathodically more active than $Mg_{65}Zn_{30}Ca_5$. The corrosion current densities which is proportional to the general corrosion rate, deduced from the intersection of cathodic Tafel line and corrosion potential are 6.6×10^{-6}, 3.5×10^{-6} and 1.9×10^{-5} A/cm^2 for $Mg_{65}Zn_{30}Ca_5$, $Mg_{65}Zn_{30}Ca_4Ag_1$ and $Mg_{63}Zn_{30}Ca_4Ag_3$, respectively. The polarization resistances can be deduced from anodic and cathodic Tafel lines as well as corrosion potential in polarization curves by Stern–Geary equation $R_p = b_a \cdot b_c / 2.3(b_a + b_c) i_{corr}$, where R_p is polarization resistance, b_a and b_c are the slopes of the anodic and cathodic Tafel, i_{corr} is corrosion current density [16]. After calculating, the polarization resistances of high purity Mg, $Mg_{65}Zn_{30}Ca_5$, $Mg_{65}Zn_{30}Ca_4Ag_1$ and $Mg_{63}Zn_{30}Ca_4Ag_3$ are presented in Fig. 4. The $Mg_{65}Zn_{30}Ca_4Ag_1$ has a higher value of 8542 Ohms/cm^2, in contrast to 5710 Ohms/cm^2 for high purity Mg, 5640 Ohms/cm^2 for $Mg_{65}Zn_{30}Ca_5$ and 4125 Ohms/cm^2 for $Mg_{63}Zn_{30}Ca_4Ag_3$.

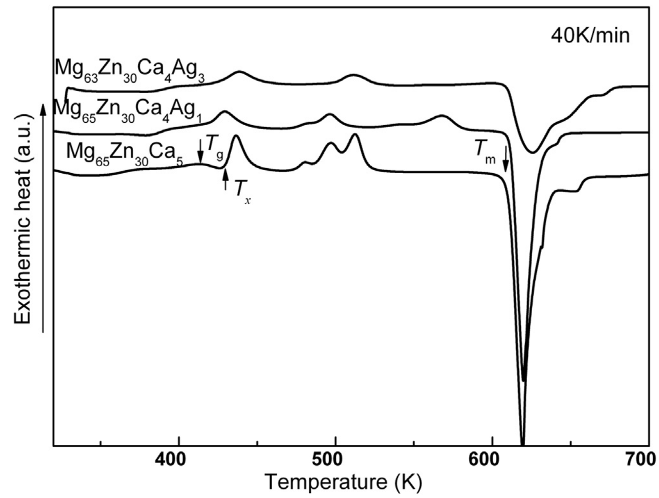

Fig. 2. DSC curves of the as-spun $Mg_{65}Zn_{30}Ca_5$, $Mg_{65}Zn_{30}Ca_4Ag_1$ and $Mg_{63}Zn_{30}Ca_4Ag_3$ amorphous alloys.

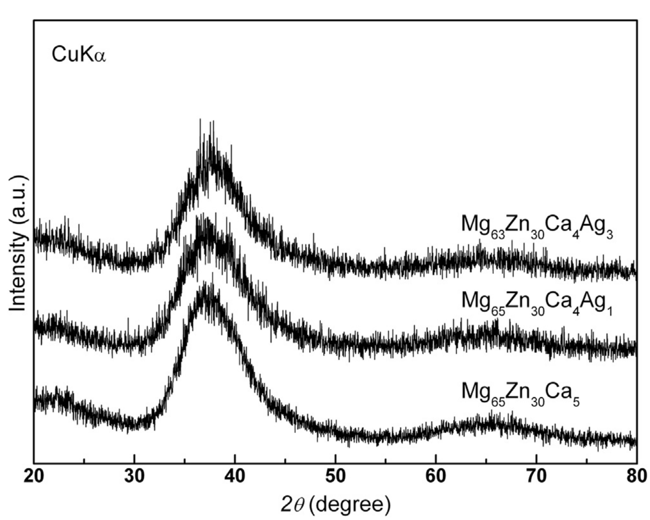

Fig. 1. XRD patterns of the as-spun $Mg_{65}Zn_{30}Ca_5$, $Mg_{65}Zn_{30}Ca_4Ag_1$ and $Mg_{63}Zn_{30}Ca_4Ag_3$ amorphous alloys.

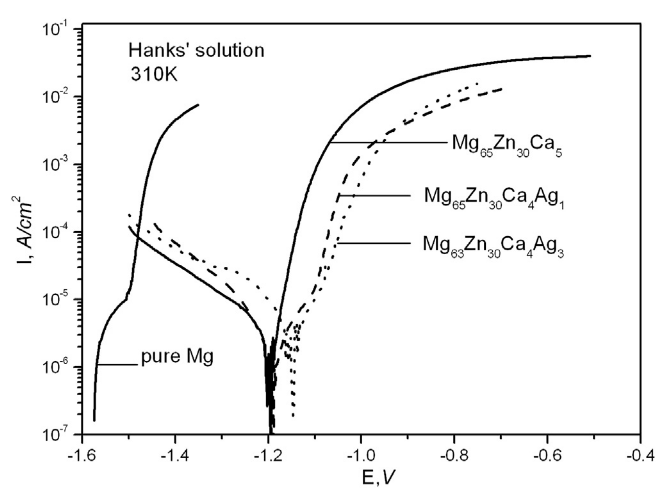

Fig. 3. Potentiodynamic polarization curves of the as-spun $Mg_{65}Zn_{30}Ca_5$, $Mg_{65}Zn_{30}Ca_4Ag_1$ and $Mg_{63}Zn_{30}Ca_4Ag_3$ amorphous alloys and high purity Mg.